

Unsupervised Segmentation in Hyperspectral Images

Juntang Wang¹ Dimitris Floros² Nikos Pitsianis³ Xiaobai Sun²

¹Duke Kunshan University, China

²Duke University, USA

³Aristotle University of Thessaloniki, Greece

Abstract

Hyperspectral images (HSIs) capture both the spatial and spectral properties of materials, with broad applications in agriculture, climate studies, remote sensing and monitoring, and medical diagnostics. Unsupervised clustering in HSIs is critical for recognizing or discovering latent patterns without relying on prior labels or limited training data. However, traditional methods are challenged by the high dimensionality, spectral and spatial variability, and noises typically associated with HSIs. This study explores the use of 'BlueRed,' a graph-affiliated methodology designed to effectively address these challenges. BlueRed significantly outperforms traditional approaches such as K-Means, GMM, DBSCAN, and Spectral Clustering, setting a new standard in HSI clustering.

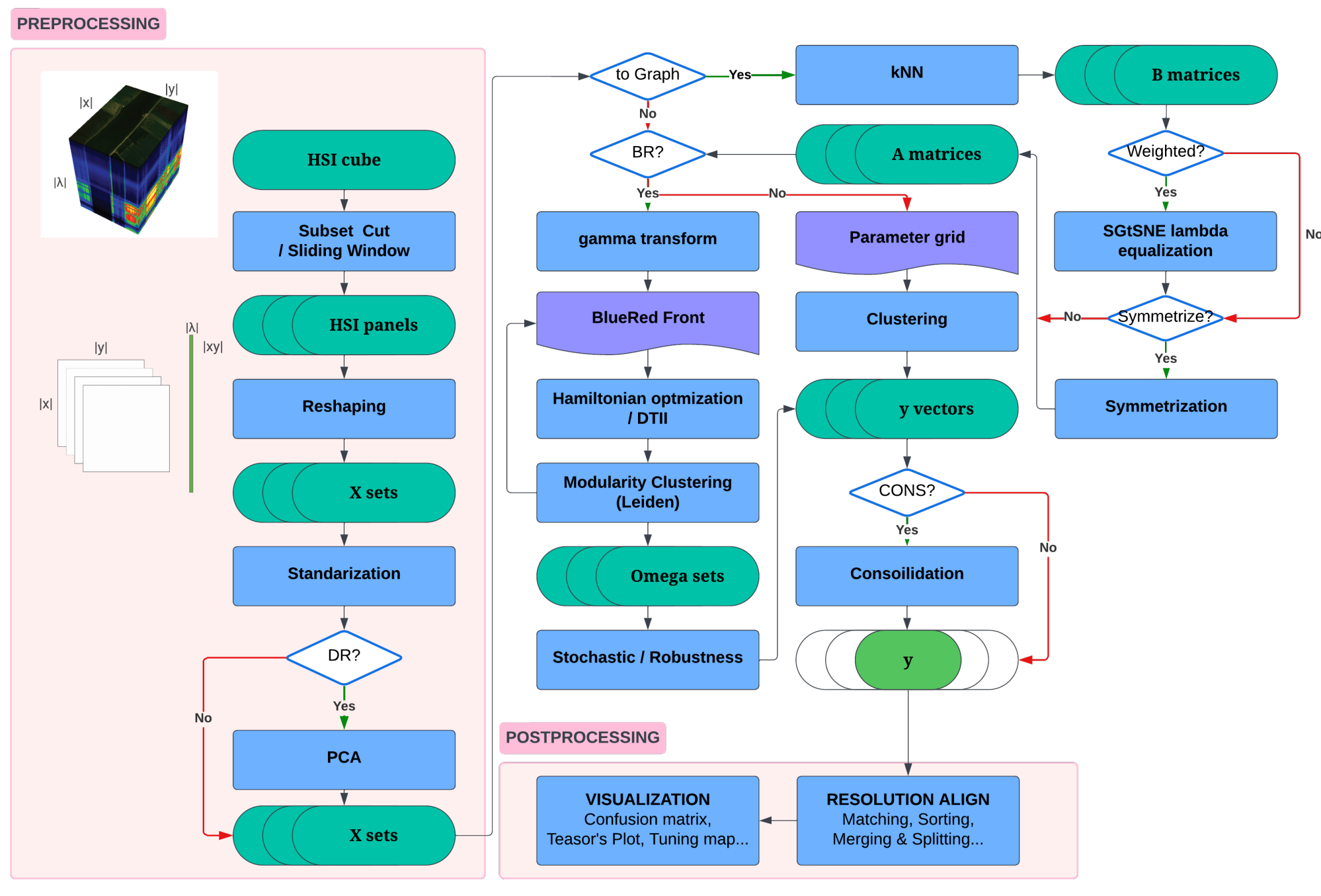


Figure 1. Flowchart of our work.

Challenges in Hyperspectral Imaging

Some main problems in hyperspectral imaging are:

- **Curse of Dimensionality:** As dimensionality increases, the unit sphere volume decreases after a certain dimension making density, distance metrics and possibility distribution less meaningful.
- **Sensitivity to Noise:** All data have noise, even low-dimensional ones, which can significantly affect clustering results.
- **Non-Convex Shapes:** Many real-world data are in non-convex shape which point-based methods may not handle effectively.
- **Parameter Sensitivity:** Methods like K-means require prior knowledge of the number of clusters, and DBSCAN relies on parameters like epsilon and minimum points, which are challenging to set appropriately for HSI data, and most likely are not uniform for any datasets.

Comparison of Clustering Methods

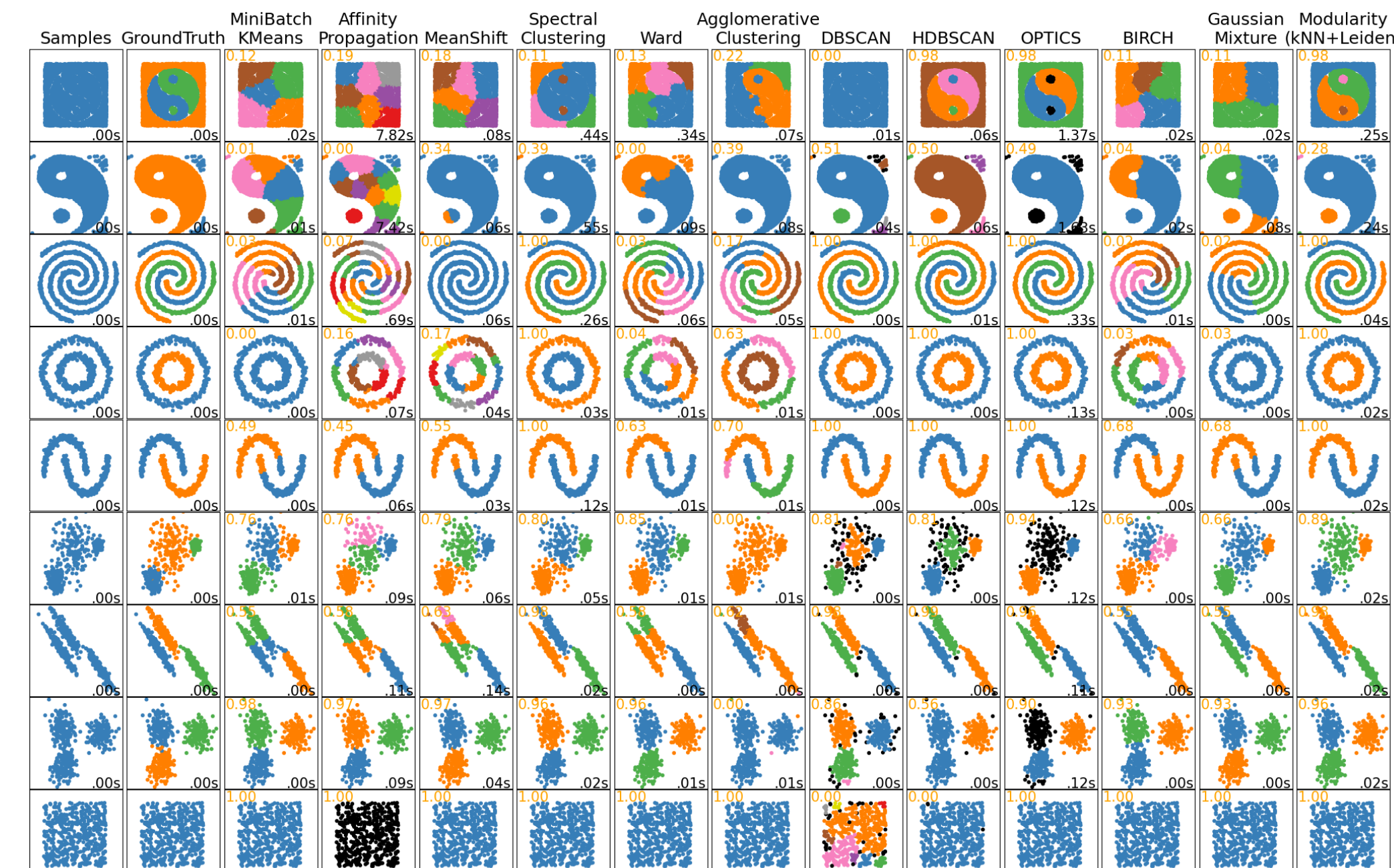


Figure 2. A comparison of Clustering Methods in scikit-learn [1] and Modularity Method. (orange) denotes ARI, (black) denotes running time.

Modularity Method (kNN + Leiden)

Drawing idea from Shi and Malik's normalized cuts [7], data points are represented as nodes within a weighted, undirected graph $G = (V, E)$, where V is the set of nodes (data points) and E is the set of edges connecting the nodes. The weight $w(i, j)$ of an edge between nodes i and j reflects their similarity.

- **k-Nearest Neighbors (kNN):** We use knn graphs for non-uniformly distributed data, latent-manifold structure, and modest integer value for k , as it capture the variance, maintain local connectivity and allow information to propagate along geodesic path, and allows easy locating of k . While a rNN graph can be dense or/and overly disconnected.
- **SG-t-SNE λ equalization:** Conversion from distance $d(x, y)$ to the edge weight $w(x, y)$ is done as follows,

$$w(x, y) = \frac{1}{\lambda} \exp(-d^2(x, y)/2\sigma_x^2), x, y \in X, (x, y) \in E(G) \quad (1)$$

where λ adjust or normalize the weight range. The non-linear scaling with σ_x is chosen to be adaptive and determined by the following sparse equations,

$$\sum_y : (x, y) \exp(-d^2(x, y)/(2\sigma_x^2)) = \lambda, x \in X \quad (2)$$

The adjacency matrix then is column stochastic

▪ **Leiden:** Then we run Leiden [8] with a modularity parameter γ .

Real-world Datasets Used in this Study

Table 1 summarizes the hyperspectral datasets utilized in our experiments. These datasets predominantly originate from the remote sensing domain and present a variety of challenges, including differing spatial resolutions, spectral ranges, and class complexities.

Table 1. Summary of Hyperspectral Datasets

Dataset	#x	#y	#λ	λ (nm)	#C	Res. (m)	Year	Platform	Source
Indian Pines	145	145	200	400-2500	16	20	1992	Air	[2]
KSC	512	614	176	400-2500	13	18	1996	Air	[5]
Salinas	512	217	204	400-2500	16	3.7	N/A	Air	[5]
Salinas-A	86	83	204	400-2500	6	3.7	N/A	Air	[5]
Botswana	1476	256	145	400-2500	14	30	2001	Space	[5]
Pavia	1096	715	102	430-860	9	1.3	N/A	Air	[5]
Pavia University	610	340	103	430-860	9	1.3	N/A	Air	[5]
WHU-Hi-HanChuan	1217	303	274	400-1000	16	0.109	2016	UAV	[9], [10]
WHU-Hi-HongHu	940	475	270	400-1000	22	0.043	2017	UAV	[9], [10]
WHU-Hi-LongKou	550	400	270	400-1000	9	0.463	2018	UAV	[9], [10]
BigEarthNet-S2-s	1200	1200	12	443-2190	11	10, 20, 60	2017	Space	[3], [6]



Figure 3. Example visualizations of some real-world datasets used in this study. (Rows from up to down) BigEarthNet-S2-s, Indian Pines, Salinas-A, Pavia, WHU-Hi-LongKou. (Columns from left to right) approximate true color images (TCIs), false color images (FCIs), ground truth (GT).

General Methodology (An Example of Pipeline)

Here we showcase an example from the pipeline, applying the GMM method on the Salinas-A dataset. This example demonstrates our postprocessing and visualization tools, which include matching, sorting, merging, and splitting of clusters. Specifically, it shows the merging of clusters 21 and 10, optimizing local recall and precision.

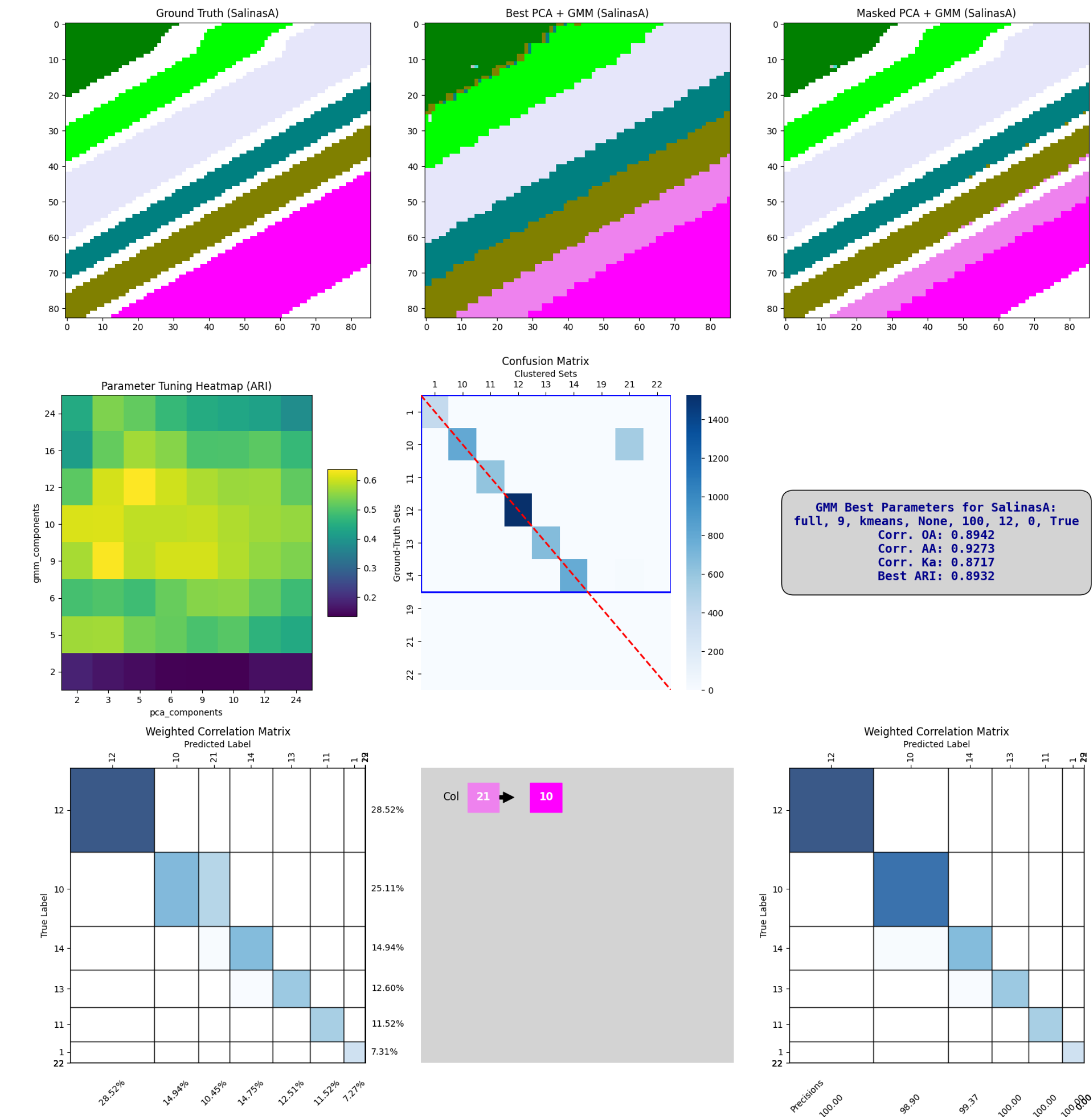


Figure 4. Example output from the pipeline for the Salinas-A dataset. The figure shows the ground truth, best and masked PCA + GMM results, parameter tuning heatmap, confusion matrix, and weighted correlation matrices.

Preliminary Results

Table 2. Performance of Unsupervised Clustering Methods on Hyperspectral Datasets (min Precisions and min Recalls)

Dataset	K-Means	GMM	DBSCAN	HDBSCAN	Spectral	kNN-Leiden	γ	BlueRed	Ω
Indian Pines	0.74	0.00	19.60	35.97	53.34	28.77	1.108	0.00	11.08
KSC	33.28	37.12	43.57	87	207.78	65.77	0.00	52.28	0.25
Salinas	44.1	50.00	50.00	50.00	50.00	50.00	0.00	41.22	0.25
Salinas-A	1.41	30.42	31.41	91.49	93.99	80.05	82.16	88.15	91.84
Botswana	29.21	42.36	67.19	44.21	0.00	73.42	0.00	30.50	71.20
Pavia	69.21	34.97	49.40	47.76	43.38	40.44	94.18	52.15	57.08
PaviaU	44.05	51.35	46.03	29.07	77.69	53.73	0.00	74.75	37.16
WHU-Hi-HanChuan	74.82	81.54	86.04	42.76	99.99	44.82	99.99	70.84	94.71
WHU-Hi-HongHu	74.98	86.05	77.31	80.05	99.99	28.11	99.99	76.34	14.52
WHU-Hi-LongKou	99.98	69.35	99.99	69.35	98.32	69.35	99.73	69.35	75.36
BigEarthNet-S2-s	34.76	49.95	33.24	47.58	65.06	65.39	0.00	74.32	0.5

Pre. Rec.

BlueRed

Hamiltonian Optimization for Graph Community Detection:

$$H(S) = \sum_{i,j \in V} A_{ij} \delta(S_i, S_j) - \gamma \sum_{i,j \in V} A_{ij} \delta(S_i, S_j), \quad (3)$$

▪ **γ Transformation:** With the help of developed theory, we map $\gamma \in [0, \infty)$ to a bounded parameter $\theta \in [0, 1]$ using a smooth transformation. One possible transformations is the sigmoid transformation:

$$\theta(\gamma) = \frac{1}{1 + e^{-\alpha(\gamma-\beta)}}, \quad (4)$$

▪ **Descending Triangular (Dimitris-Tiancheng):** To prioritize finer community structures during optimization, a descending triangular weighting function can be used:

$$w(\theta) = \begin{cases} 1 - 2\theta & \text{if } 0 \leq \theta \leq 0.5, \\ 2\theta - 1 & \text{if } 0.5 < \theta \leq 1. \end{cases} \quad (5)$$

The detailed BlueRed algorithm is temporarily withheld before disclosure. Below is an example figure from a related work by Dimitrios et al., illustrating a segmented image.



Figure 5. (a) Santorini HD image (b) Segmented image from related work by Dimitrios et al. [4]

Acknowledgements

I would like to express my gratitude to the author group: Dimitris Floros, Nikos Pitsianis, and Xiaobai Sun, for their guidance. Special thanks to my mentor, Prof. Shixin Xu, for his mentorship, and heartfelt appreciation to Yihan Wang and my mother for their unwavering support. This project was funded by the Office of Academic Services and the DKU Student Experimental Learning Fellowship (SELF) Program.

References

- [1] 2.3. Clustering. scikit-learn. URL: <https://scikit-learn/stable/modules/clustering.html> (visited on 08/05/2024).
- [2] M. Baumgardner, L. Biehl, and D. Landgrebe. 220 Band AVIRIS Hyperspectral Image Data Set: June 12, 1992 Indian Pine Test Site 3. Version 1.0. Purdue University Research Repository, 2015.
- [3] K. N. Clasen, L. Hackel, T. Burgert, G. Sumbul, B. Demir, and V. Markl. "reBEN: Refined BigEarthNet Dataset for Remote Sensing Image Analysis". 2024. arXiv: 2407.03653 [cs.CV].
- [4] D. Floros, T. Liu, N. Pitsianis, and X. Sun. "Sparse Dual of the Density Peaks Algorithm for Cluster Analysis of High-dimensional Data". In: 2018 IEEE High Performance Extreme Computing Conference (HPEC). 2018 IEEE High Performance Extreme Computing Conference (HPEC). Waltham, MA: IEEE, Sept. 2018, pp. 1–14.
- [5] M. Grana, M. A. Veganzons, and B. Ayerdi. Hyperspectral Remote Sensing Scenes. Grupo de Inteligencia Computacional (GIC). 2020. URL: https://www.ehu.eus/ccwintco/index.php/Hyperspectral_Remote_Sensing_Scenes.
- [6] L. Hackel, K. N. Clasen, and B. Demir. "ConfigILM: A General Purpose Configurable Library for Combining Image and Language Models for Visual Question Answering". In: SoftwareX 26 (2024), p. 101731.
- [7] Jianbo Shi and J. Malik. "Normalized Cuts and Image Segmentation". In: IEEE Transactions on Pattern Analysis and Machine Intelligence 22.8 (Aug./2000), pp. 888–905.
- [8] V. A. Traag, L. Waltman, and N. J. Van Eck. "From Louvain to Leiden: Guaranteeing Well-Connected Communities". In: Scientific Reports 9.1 (Mar. 26, 2019), p. 5233.
- [9] Y. Zhong, X. Hu, C. Luo, X. Wang, J. Zhao, and L. Zhang. "WHU-Hi: UAV-borne Hyperspectral with High Spatial Resolution (H2) Benchmark Datasets and Classifier for Precise Crop Identification Based on Deep Convolutional Neural Network with CRF". In: Remote Sensing of Environment 250 (Dec. 2020), p. 112012.
- [10] Y. Zhong, X. Wang, Y. Xu, S. Wang, T. Jia, X. Hu, J. Zhao, L. Wei, and L. Zhang. "Mini-UAV-Borne Hyperspectral Remote Sensing: From Observation and Processing to Applications". In: IEEE Geoscience and Remote Sensing Magazine 6.4 (Dec. 2018), pp. 46–62.